

Applying GMDH neural network to estimate the thermal resistance and thermal conductivity of pulsating heat pipes

Mohammad Hossein Ahmadi, Milad Sadeghzadeh, Amir Hossein Raffiee & Kwok-wing Chau

To cite this article: Mohammad Hossein Ahmadi, Milad Sadeghzadeh, Amir Hossein Raffiee & Kwok-wing Chau (2019) Applying GMDH neural network to estimate the thermal resistance and thermal conductivity of pulsating heat pipes, Engineering Applications of Computational Fluid Mechanics, 13:1, 327-336, DOI: [10.1080/19942060.2019.1582109](https://doi.org/10.1080/19942060.2019.1582109)

To link to this article: <https://doi.org/10.1080/19942060.2019.1582109>



© 2019 The Author(s). Published by Informa UK Limited, trading as Taylor & Francis Group



Published online: 12 Mar 2019.



Submit your article to this journal [↗](#)



Article views: 175



View Crossmark data [↗](#)

Applying GMDH neural network to estimate the thermal resistance and thermal conductivity of pulsating heat pipes

Mohammad Hossein Ahmadi^a, Milad Sadeghzadeh^b, Amir Hossein Raffiee^c and Kwok-wing Chau^d

^aFaculty of Mechanical Engineering, Shahrood University of Technology, Shahrood, Iran; ^bRenewable Energy and Environmental Engineering Dep., University of Tehran, Tehran, Iran; ^cSchool of Mechanical Engineering, Purdue University, West Lafayette, IN, USA; ^dDepartment of Civil and Environmental Engineering, Hong Kong Polytechnic University, Hong Kong, People's Republic of China

ABSTRACT

Thermal performance of pulsating heat pipes (PHPs) is dependent to several factors. Inner and outer diameter of tube, filling ratio, thermal conductivity, heat input, inclination angle, and length of each section are the most influential factors in the design process of PHPs. Since water is a conventional working fluid for PHPs, thermal resistance and effective thermal conductivity of PHPs filled with water are modeled by applying a GMDH (group method of data handling) neural network. The input data of the GMDH model are collected from other experimental investigations to predict the physical properties including thermal resistance and effective thermal conductivity of PHPs filled with water as working fluid. The accuracy of the introduced models are examined through the R^2 tests and resulted in 0.9779 and 0.9906 for thermal resistance and effective thermal conductivity, respectively.

ARTICLE HISTORY

Received 28 December 2018
Accepted 9 February 2019

KEYWORDS

Pulsating heat pipe; thermal resistance; effective thermal conductivity; GMDH

1. Introduction

Reduction in the size of various devices makes it necessary to have more effective cooling methods. One efficient cooling device is the heat pipe. Heat pipes are passive cooling devices consisting of a tube and partially filled with working fluid (Faghri, 1995). Two-phase heat transfer is the main reason for higher heat transfer effectiveness in pulsating heat pipes (PHPs) (Buffone, Sefiane, Buffone, & Lin, 2005). The working fluid in heat pipes receives heat in the evaporator section and evaporates, and returns to its liquid condition by heat dissipation in the condenser section. In addition to the evaporator and condenser, an optional adiabatic section exists in heat pipes when there is gap between the heat source and heat sink. Heat pipes' characteristics such as high heat transfer capacity make them a good choice for use in several thermal systems (Motahar & Khodabandeh, 2016).

Several classes of heat pipes have been introduced so far, such as wick, rotating, and pulsating heat pipes (Alizadeh et al., 2018; Ramezanizadeh et al., n.d.). The fluid exchange between the condenser and the evaporator is caused by the capillary force in the wick type. Rotating heat pipes use centrifugal force for this purpose. Pressure instabilities move the fluid in PHPs; in addition, gravity helps fluid motion where the evaporator section is located at the bottom.

PHPs can be built more compact than other classes of heat pipes (Alhuyi Nazari, Ghasempour, Ahmadi, Heydarian, & Shafii, 2018). PHPs are formed of a capillary tube. This tube is bent in various arrangements as shown in Figure 1 (Gandomkar, Saidi, Shafii, Vandadi, & Kalan, 2017; Mohammadi, Mohammadi, & Shafii, 2012). PHPs can be used for different applications such as electronic device cooling, water heating systems, desalination systems, heat transfer improvement in phase change material (PCM), and renewable energy (Alhuyi Nazari, Ahmadi, Ghasempour, & Shafii, 2018). Thermal performance of PHPs is influenced by several design variables including heat input, geometry, material of tube, inclination angle, inner and outer diameter, working fluid, etc. (Zamani, Kalan, & Shafii, 2018). Increase in the heat input, before dry-out, results in a higher rate of fluid vaporization, which means an increase in boiling heat transfer. Geometries with the ability to facilitate fluid motion are more favorable. Connecting the channels and utilizing pipes with various sizes are among the suggestions to achieve better fluid circulation inside PHPs (Ebrahimi, Shafii, & Bijarchi, 2015). In addition, higher thermal conductivity of PHP wall leads to better heat transfer in both radial and axial heat transfer. The influence of inclination angle is attributed to its impact on the gravitational force that affects the fluid flow.

CONTACT Mohammad Hossein Ahmadi  mhosein.ahmadi@shahroodut.ac.ir, mohammadhosein.ahmadi@gmail.com

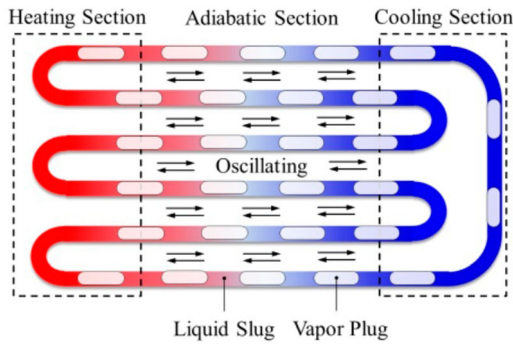


Figure 1. Schematic of a PHP (Daimaru, Yoshida, & Nagai, 2017).

System identification approaches have the ability to estimate and forecast the performances of compound devices on the basis of specified input–output (Faizollahzadeh Ardabili et al., 2018; Moazenzadeh, Mohammadi, Shamshirband, & Chau, 2018; Ramezanizadeh, Ahmadi, Ahmadi, & Alhuyi Nazari, 2018). Various calculation methods have been applied for this purpose including fuzzy logic, neural network (NN), and evolutionary algorithms (Baghban, Jalali, Shafiee, Ahmadi, & Chau, 2019; Wu & Chau, 2011). By applying these methods, it is possible to improve understanding and issues in complex and non-linear systems.

Several methods and algorithms have been used to recognize systems' behavior and estimate their performance (Hemmat Esfe, Tatar, Ahangar, & Rostamian, 2018; Taormina, Chau, & Sivakumar, 2015; Yaseen, Sulaiman, Deo, & Chau, 2019). A novel analysis approach that is multivariate is GMDH (group method of data handling), which was introduced by Ivakhnenko (Ahmadi, Ahmadi, Mehrpooya, & Rosen, 2015) in order to model complicated systems. GMDH is applied to avoid the difficulty of obtaining data when using the mathematical method of evolution. Hence, by applying GMDH it is possible to demonstrate complex systems when some of the systems' specifications are not given.

GMDH produces an analytical function in a feed-forward network based on a quadratic node transfer function (Rezaei, Sadeghzadeh, Alhuyi Nazari, Ahmadi, & Astaraei, 2018). In this function, the constraints are acquired by a regression procedure. The use of self-organizing networks results in higher effectiveness of the GMDH method for several applications (Rezaei et al., 2018).

Since the performance of PHPs depends on different factors, it is very complicated to evaluate the impact of each factor by means of experimental studies. Moreover, due to the chaotic behavior of PHPs, numerical modeling of them using computational fluid dynamic is very difficult. Due to the facts mentioned, a comprehensive

approach must be used to accurately predict the thermal performance of PHPs and consider all the factors influencing their heat transfer. The use of artificial neural network (ANN) to estimate the thermal resistance of PHPs by consideration of different factors is introduced as a novel idea. In this study, a model is proposed incorporating results of experimental studies on PHPs and the GMDH method. The obtained results are verified against actual data that are obtained experimentally. In order to consider all of the factors, 315 data are extracted from various studies (Cui, Zhu, Li, & Shun, 2014; Jia, Jia, & Tan, 2013; Li & Yan, 2008; Lin, Kang, & Chen, 2008; Mameli, Manno, Filippeschi, & Marengo, 2014; Qu & Wang, 2013; Saha, Das, & Sharma, 2014; Shafii, Arabnejad, Saboohi, & Jamshidi, 2010; Wang, Lin, Zhang, Chen, & Tang, 2009; Wang, Ma, Zhu, Dong, & Yue, 2016; Zhao, Zhao, & Ma, 2013; Zhu, Cui, Han, & Sun, 2014). The polynomial NN and the resulted estimations are trained by the gathered data. The model inputs are inner and outer diameter, tube thermal conductivity, turns, lengths of different sections (adiabatic, evaporator, and condenser), heat input, filling ration, and sine of inclination angle while the physical features of thermal resistance and effective thermal conductivity are defined as the outputs of the model. Since one of the most applicable working fluids in PHPs is water, which has shown appropriate heat transfer ability in PHPs, all the investigated heat pipes work with water as working fluid. A GMDH-style NN is applied in order to determine the relationship between inputs and outputs based on polynomials. This NN evolutionary algorithm needs optimization methods in order to define the best topology for the network. So the genetic algorithm is employed to determine the topology in an innovative procedure, i.e. the number of neurons in the hidden layers and their specific linking arrangements. Singular value decomposition (SVD) is utilized to obtain the optimal values of the constants in the equations applied for modeling thermal resistance and thermal conductivity (Ahmadi et al., 2015).

2. GMDH principles

The underlying principle behind GMDH can be readily described as the association of various pairs throughout every layer by means of quadratic polynomials using the GMDH algorithm, and thereby the generation of new-born neurons for the subsequent layer. These valuable findings have this potential to be employed to tie inputs to outputs in modeling. Although there are a number of definition for the recognition issue, the accepted one is to specify an \hat{f} function, which is the approximate estimation of the actual function of f for a close prediction of \hat{y} to y for the specific input $X = (x_1, x_2, x_3, \dots, x_n)$. For a

number of M observations the actual output is (Ahmadi et al., 2015):

$$y_i = f(x_{i1}, x_{i2}, x_{i3}, \dots, x_{in}) \quad (i = 1, 2, 3, \dots, M) \quad (1)$$

A GMDH NN can now be used to predict the target values \hat{f}_i for any particular input vector $X = (x_{i1}, x_{i2}, x_{i3}, \dots, x_{in})$ as:

$$\hat{y}_i = \hat{f}(x_{i1}, x_{i2}, x_{i3}, \dots, x_{in}) \quad (i = 1, 2, 3, \dots, M) \quad (2)$$

Then, we need to specify a GMDH NN to obtain the minimum square difference values of the real targets and the determined ones:

$$\sum_{i=1}^M [\hat{f}(x_{i1}, x_{i2}, x_{i3}, \dots, x_{in}) - \hat{y}_i]^2 \rightarrow \min \quad (3)$$

A discrete practice of the Volterra functional (Farlow & Farlow, 1984; Ivakhnenko, 1971; Nariman-Zadeh, Darvizeh, Felezi, & Gharababaei, 2002) series can be used to constitute the general equation to obtain the output directly through inputs as follows (Ahmadi et al., 2015):

$$y = a_0 + \sum_{i=1}^n a_i x_i + \sum_{i=1}^n \sum_{j=1}^n a_{ij} x_i x_j + \sum_{i=1}^n \sum_{j=1}^n \sum_{k=1}^n a_{ijk} x_i x_j x_k + \dots \quad (4)$$

Equation (4) is identified as the Kolmogorov–Gabor polynomial. A complex of partial quadratic polynomials consisting of two factors (neurons) can represent this full algebraic arrangement, i.e.:

$$\hat{y} = G(x_i, x_j) = a_0 + a_1 x_i + a_2 x_j + a_3 x_i^2 + a_4 x_j^2 + a_5 x_i x_j \quad (5)$$

In this respect, a partial quadratic layout is applied in a reverse sequence in every part of a linked-neurons network in order to assemble the overall correlation of input–output which is described in Equation (4). Regression approaches are utilized to specify the coefficients a_i in Equation (5) for each set of inputs x_i and x_j , with the intention of making the real output y close to the forecasted \hat{y} (Ahmadi et al., 2015).

It can be perceived that employing the quadratic form presented in Equation (5) results in a hierarchy of polynomials. The constants of the polynomials are obtained through a least-squares approach. Next, the G_i constants are acquired with the aim of optimally fitting the outputs,

as follows, for the total set of input–output (Ahmadi et al., 2015):

$$E = \frac{\sum_i^M (y_i - G_i)^2}{M} \rightarrow \min$$

In the GMDH approach, two independent factors from the total n input are chosen to provide the probabilities. In fact, this is accomplished by developing the regression polynomial in Equation (5), which closely follows the observations $(y_i, i = 1, 2, \dots, M)$ by a least-squares method.

The number of $\binom{n}{2} = \frac{n(n-2)}{2}$ neurons are gathered from the major hidden layer of the feed forward NN from the M observations $\{(y_i, x_{ip}, x_{iq}); (i = 1, 2, \dots, M)\}$ for a variety of $p, q \in \{1, 2, \dots, n\}$ which are now favorable to form triple data sets of $\{(y_i, x_{ip}, x_{iq}); (i = 1, 2, \dots, M)\}$ from observations using $p, q \in \{1, 2, \dots, n\}$ sets (Ahmadi et al., 2015):

$$\begin{bmatrix} x_{1p} & x_{1q} & y_1 \\ x_{2p} & x_{2q} & y_2 \\ x_{3p} & x_{3q} & y_m \end{bmatrix}$$

The succeeding matrix can be immediately obtained by applying the quadratic sub-formulation type of Equation (5) for every row of M triple data sets:

$$Aa = Y \quad (6)$$

$$a = \{a_0, a_1, a_2, a_3, a_4, a_5\} \quad (7)$$

$$Y = \{y_1, y_2, y_3, \dots, y_M\}^T \quad (8)$$

where a represents the vector of unknown constants for the quadratic polynomial in Equation (5), and Y is the output. Hence, it is shaped as follows:

$$\begin{bmatrix} 1 & x_{1p} & x_{1q} & x_{1p}x_{1q} & x_{1p}^2 & x_{1q}^2 \\ 1 & x_{2p} & x_{2q} & x_{2p}x_{2q} & x_{2p}^2 & x_{2q}^2 \\ \dots & \dots & \dots & \dots & \dots & \dots \\ 1 & x_{Mp} & x_{Mq} & x_{Mp}x_{Mq} & x_{Mp}^2 & x_{Mq}^2 \end{bmatrix} \quad (9)$$

The following equation is a result of utilizing the least-squares method from analyzing of the multiple-regression influence:

$$a = (A^T A)^{-1} A^T Y \quad (10)$$

Equation (10) is used to obtain the optimal values of used constants in Equation (5) for the total array of M triple data sets. All of the neurons which are placed in the next hidden layer are escorted by the connectivity configuration of the NN. This procedure is repeated. The obtained results are precisely accessible to enhance deviations and, more notably, to intensify the uniqueness of

above equations (Ali Ahmadi & Golshadi, 2012; Jamali, Nariman-Zadeh, Darvizeh, Masoumi, & Hamrang, 2009; Lin, Cheng, & Chau, 2006; Nariman-zadeh, Atashkari, Jamali, Pilechi, & Yao, 2005).

The primary fundamentals of a GMDH NN are topology determination and the Ali Ahmadi genetic algorithm that is employed in the process of designing the GMDH NNs. Since stochastic techniques have been effectively applied and confirmed to be better than typical gradient-based techniques in terms of finding connected coefficients or weights of NNs, they are commonly employed in the procedure of training NNs.

Neurons of any layer, in most GMDH-style NNs, are associated with a neuron in a nearby layer, as has previously been explained (Ali Ahmadi & Golshadi, 2012; Nariman-zadeh, Atashkari, Jamali, Pilechi, & Yao, 2005). This improvement results in the use of a straightforward programming pattern, demonstrated in Figure 2, for each genotype, as was earlier proposed (Nariman-zadeh et al., 2005; Yao, 1999).

GMDH NNs (generalize the structure of group method of data handling [GS-GMDH]) must be capable of illustrating NNs of any length and size. As illustrated in Figure 1, throughout a GS-GMDH NN, *ad* inside the primary hidden layer is directly involved with the output layer by covering the hidden layer of the next stage. Therefore, it can be perceived that the output of *abccadad* consists of double *ad*. A cybernetic neuron of *adad* is formed in the hidden layer of the next stage and used in the same layer to assemble the output, as demonstrated in the Figure 1 (Ahmadi et al., 2015).

The procedure is started when a neuron is delivered to specified adjacent hidden layers and links to another neuron in the subsequent hidden layer (second, or third, or fourth, and so on). In this modeling pattern, the number of repetitions is $2^{\tilde{n}}$, where \tilde{n} indicates the number of hidden layers. It should be noted that the chromosomes of *ababbcbc* and *ababacbc* are different, and thereby it is not a separate function in the GS-GMDH networks and has to be directly revised as *abbc*.

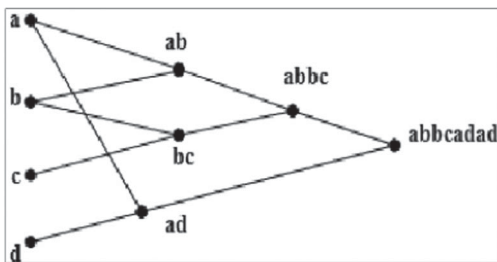


Figure 2. Network structure of chromosomes in GMDH (Ahmadi et al., 2015).

Applying the GA mutation and crossover operatives makes it possible to create two children from a father and a mother. In this regard, to find out the parents of the two children, an ordinary roulette wheel selection technique is utilized (Nariman-zadeh et al., 2005; Yao, 1999).

Every network is monitored by a prolonged string in order to form the GMDH NNs. To characterize a GMDH-style NN approach, the fitness (ϕ) of each string is calculated as follows:

$$\phi = \frac{1}{E} \quad (11)$$

where E denotes the mean square error (MSE) in Equation (10), which is minimized by using the fitness factor of ϕ in the evolutionary algorithm.

The evolutionary algorithm is commenced by selecting an arbitrary values from the population. Next, mutation, crossover, and roulette wheel, the genetic operators, are applied on the whole population of illustrative series to gradually improve the solution. GMDH NN techniques with dramatically increasing fitness factor are developed until the progress comes to an acceptable level.

The precision of the presented polynomial models are assessed and evaluated through several methods such as correlation of determination (R^2), and root mean square error (RMSE), and mean absolute percentage of error (MAPE) (Bildirici & Ersin, 2014; Elçiçek, Akdoğan, & Karagöz, 2014; Gonzalez-Sanchez, Frausto-Solis, & Ojeda-Bustamante, 2014):

$$R^2 = 1 - \left[\frac{\sum_{i=0}^M (Y_{i(\text{model})} - Y_{i(\text{actual})})^2}{\sum_{i=1}^M (Y_{i(\text{actual})})^2} \right] \quad (12)$$

$$RMSE = \left[\frac{\sum_{i=0}^M (Y_{i(\text{model})} - Y_{i(\text{actual})})^2}{M} \right]^{\frac{1}{2}} \quad (13)$$

$$MAPE = \left[\frac{\sum_{i=0}^M |Y_{i(\text{model})} - Y_{i(\text{actual})}|}{M \sum_{i=1}^M Y_{i(\text{actual})}} \right] \quad (14)$$

3. Results and discussion

In this study, the thermal resistance and thermal conductivity of PHPs filled with water as working fluid are determined by applying a GMDH method. Various effective parameters' effect on thermal resistance and thermal performance are considered. The parameters are inner and outer diameter of tube, number of turns, lengths of evaporator, condenser, and adiabatic sections, thermal conductivity of tube material, inclination angle of PHP, filling ratio, and heat input. In order to calculate the effective thermal conductivity of the PHP, Equations (15) and

(16) are applied.

$$l_{eff} = l_{ad} + 1/2(l_e + l_c) \quad (15)$$

$$K_{eff} = l_{eff}/R.A_{PHP} \quad (16)$$

Data are extracted from several studies in order to represent a comprehensive model that is applicable for various working conditions. Based on the approach described, the polynomials generated for thermal resistance (Equation [17]) and effective thermal conductivity (Equation [18]) are as follows:

$$\begin{aligned} \text{thermal resistance} &= 1.3793 - di * 1.86534 + di^2 * \\ &0.584331 + N2 * 1.026 - N2^2 * 0.00145972 \\ N2 &= -0.0153625 + N668 * 0.0602603 + N4 * \\ &0.942843 + N4^2 * 0.00250313 \\ N4 &= -0.206913 + N938 * 0.353221 + N938 * N13 * \\ &0.0146303 - N938^2 * 0.0942794 + N13 * 0.960321 \\ N13 &= 0.0136544 - N382 * 0.25184 + N382^2 * \\ &0.00114117 + N18 * 1.23753 \\ N18 &= -0.0031026 + N61 * 0.264179 - N61 * N63 * \\ &0.695382 + N61^2 * 0.384159 + N63 * 0.729397 \\ &+ N63^2 * 0.311604 \\ N63 &= 0.0437684 - N475 * 0.564158 + N475 * N108 * \\ &1.51567 - N475^2 * 0.698669 + N108 * 1.55382 \\ &- N108^2 * 0.814698 \\ N108 &= -0.0267701 + N142 * 0.441903 - N142 * \\ &N195 * 2.14596 + N142^2 * 1.09139 + N195 * \\ &0.538925 + N195^2 * 1.05613 \\ N195 &= -0.0674541 - N762 * 0.151637 - N762 * \\ &N455 * 0.241551 + N762^2 * 0.140852 + N455 * \\ &1.23267 + N455^2 * 0.0661478 \\ N455 &= -0.0452748 + N512 * 0.592131 - N512 * \\ &N954 * 0.0309739 + N512^2 * 0.0574798 \\ &+ N954 * 0.30691 \\ N954 &= 5.00243 - N998 * 1.81918 + N998 * N1001 * \\ &3.15769 - N998 \wedge 2 * 0.267178 - N1001 * \\ &5.61491 + N1001^2 * 0.475315 \\ N1001 &= -4232.38 + \text{filling ratio} * 62821.7 \\ &- \text{filling ratio} * \text{filling ratio} * 28299.4 \\ &+ \text{filling ratio}^2 * 2641.85 + \text{filling ratio} * \end{aligned}$$

$$\begin{aligned} &25272.5 - \text{filling ratio}^2 * 58203.9 \\ N998 &= -9.02357 + lc * 1.93546 - lc * \text{angle} * \\ &2.22982 - lc^2 * 0.0646227 + \text{angle} * 12.8099 \\ &- \text{angle}^2 * 0.176741 \\ N762 &= 2.19892 - N949 * 5.12281 - N949 * \\ &N999 * 2.24318 + N949^2 * 2.55658 + N999 * \\ &4.25731 - N999^2 * 0.9546 \\ N999 &= 2.91766 - lc * 0.0293039 \\ &+ lc^2 * 7.42086e - 05 \\ N949 &= 8.24353 + la * 3.67117 - la * do * 1.49715 \\ &- la^2 * 0.186397 - do * 21.8758 + do^2 * 10.2176 \\ N142 &= -0.0488954 + N257 * 0.595073 - N257 * \\ &N501 * 0.852779 + N257^2 * 0.494999 + N501 * \\ &0.401075 + N501^2 * 0.35959 \\ N501 &= -0.122995 + N526 * 0.594386 - N526 * \\ &N606 * 1.3906 + N526^2 * 0.84123 + N606 * \\ &0.452032 + N606^2 * 0.501207 \\ N606 &= 0.465024 - N786 * 0.283021 + N786 * \\ &N830 * 0.493308 - N830 * 0.145692 + N830^2 * \\ &0.0898273 \\ N830 &= 4.29728 + la * 2.09115 + la * q * 0.297407 \\ &- la^2 * 0.377062 - q * 2.88556 + q^2 * 0.0749262 \\ N786 &= 8.51401 + lc * 0.162478 - lc * \text{turn} * \\ &0.19287 + lc^2 * 0.00149821 - \text{turn} * 12.7218 \\ &+ \text{turn}^2 * 6.37126 \\ N526 &= 0.415903 - N637 * 0.29853 + N637 * \\ &N952 * 0.345626 + N637^2 * 0.137537 \\ &- N952 * 0.348617 + N952^2 * 0.212929 \\ N952 &= -81.4928 - le * 0.126059 + le^2 * 0.00162688 \\ &+ lc * 48.2396 - lc^2 * 6.74378 \\ N637 &= 1.54277 - do * q * 0.575434 + do^2 * \\ &0.265486 + q * 0.728609 + q^2 * 0.0382402 \\ N257 &= 0.0202435 + N509 * 0.567101 - N509 * \\ &N648 * 0.202378 + N509^2 * 0.135832 + N648 * \\ &0.374981 + N648^2 * 0.0479461 \\ N648 &= -0.163185 + N847 * 2.01553 - N847 * \\ &N930 * 14.1819 + N847^2 * 7.59523 - N930 * \end{aligned}$$

$$\begin{aligned}
& 0.389653 + N930^2 * 5.86296 \\
N930 &= 22.0596 - lc * 0.0344342 + lc * do * \\
& 0.0100074 + lc^2 * 5.55762e - 05 - do * 28.6736 \\
& + do^2 * 10.2169 \\
N847 &= 1.44171 - turn * 0.527986 - turn * le * \\
& 0.00716259 + turn^2 * 0.0435464 + le * 0.0822812 \\
& - le^2 * 0.000406114 \\
N475 &= 0.0783022 + N512 * 0.53378 + N512^2 * \\
& 0.0862172 + N622 * 0.406139 - N622^2 * 0.101118 \\
N622 &= 0.432176 - N774 * 0.768196 + N774 * \\
& N972 * 0.548759 + N774^2 * 0.191911 - N972 * \\
& 1.05666 + N972^2 * 0.699157 \\
N774 &= 0.248366 - do * q * 0.0185382 + do^2 * \\
& 0.141916 + q * 0.0442287 + q^2 * 8.0383e - 07 \quad (17)
\end{aligned}$$

$$\begin{aligned}
\text{effective thermal conductivity} &= -13.7736 + N144 * \\
& 0.538576 + N184 * 0.464164 \\
N184 &= -2092.48 + N353 * 0.963642 + N353 * \\
& N817 * 1.63544e - 06 + N817 * 0.921357 - N817^2 * \\
& 3.44551e - 05 \\
N817 &= 2086.93 + N878 * N886 * 0.000144386 \\
& - N878^2 * 4.3916e - 05 + N886 * \\
& 0.0929333 - N886^2 * 1.61099e - 05 \\
N886 &= 155103 + material * 41238.5 + material * di * \\
& 180.414 - material^2 * 107.607 - di * 149067 \\
& + di^2 * 19873.4 \\
N878 &= 84504.5 - material * 59.5247 + material * \\
& la * 13.113 + material^2 * 0.0171151 \\
& - la * 39696.3 + la^2 * 4618.96 \\
N353 &= -1743.35 + N517 * 0.722103 + N517 * \\
& N745 * 1.11633e - 05 + N745 * 1.04832 \\
& - N745^2 * 3.97024e - 05 \\
N745 &= 5634.79 + lc * 226.504 - lc * do * 42.7616 \\
& + lc^2 * 0.0752415 - do * 5161.38 + do^2 * 764.177 \\
N517 &= -906.348 + angle * 2193.7 - q * 982.231 \\
& + q^2 * 380.579 \\
N144 &= 19.6363 + N374 * 0.760643 + N374 * N624 *
\end{aligned}$$

$$\begin{aligned}
& 6.79657e - 06 + N624 * 0.197119 - N624^2 * \\
& 4.11343e - 06 \\
N624 &= -930.965 - N879 * 0.135998 - N879 * \\
& N895 * 0.00088553 + N879^2 * 0.000417206 \\
& + N895 * 0.325276 + N895^2 * 0.000461109 \\
N895 &= 67435.2 - angle * 16125.1 + angle * do * \\
& 5890.05 - angle^2 * 13706 - do * 21768 \\
& + do^2 * 1623.75 \\
N879 &= 738867 + do * 83303.9 - do * di * 43941.9 \\
& - do^2 * 3766.63 - di * 1.3808e + 06 + di^2 * 600114 \\
N374 &= -1452.64 + N520 * 0.658643 + N520 * \\
& N724 * 1.49637e - 05 + N724 * 1.00848 - N724^2 * \\
& 4.03562e - 05 \\
N724 &= -2.05598e + 06 + turn * 2.93641e + 06 \\
& - turn * turn * 568528 + turn^2 * 8873.03 + turn * \\
& 5.80685e + 06 - turn^2 * 6.12671e + 06 \\
N520 &= -1082.7 + q * 20.3081 + q * 799.277 \quad (18)
\end{aligned}$$

Input and output parameters are as follows:

Filling ratio:	filling ratio
Material:	thermal conductivity of tube
Turn:	number of turns
l_e :	length of evaporator section
l_c :	length of condenser section
l_a :	length of adiabatic section
Angle:	sinus of inclination angle
d_i :	inner diameter
d_o :	outer diameter
q :	heat input
R :	thermal resistance of heat pipe
K :	thermal conductivity of heat pipe

As shown in Figure 3, the average relative deviation (ARD) of the thermal resistance is in an appropriate range. Relative deviation decreases with increasing thermal resistance, which can be attributed to more dominant conduction heat transfer in comparison with two-phase heat transfer for high thermal resistances. The relative deviation of the applied technique for calculating thermal resistance in comparison with the experimental data is shown in Figure 2. Based on the results obtained, the maximum relative error is approximately 35.8% and reaches less than 5% for thermal resistances higher than 10 K/W.

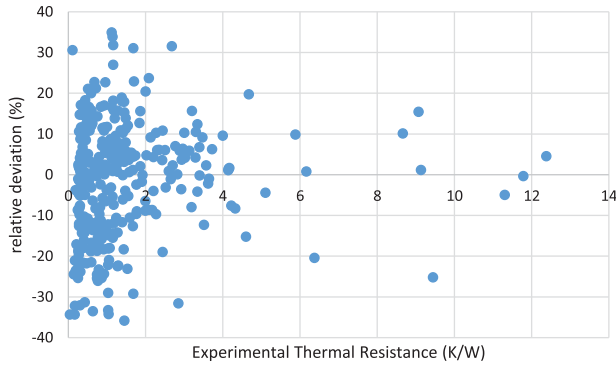


Figure 3. Relative error of thermal resistance versus experimental data.

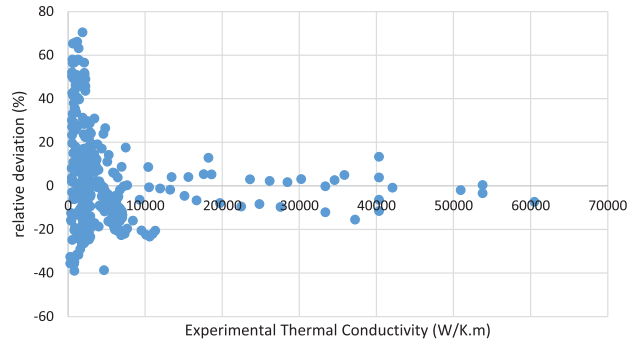


Figure 6. Relative error of effective thermal conductivity versus experimental data.

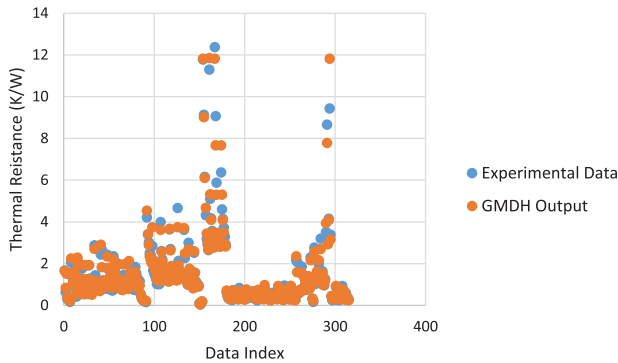


Figure 4. GMDH output versus actual data: thermal resistance.

Figure 4 shows data obtained by applying a GMDH model and compares them with actual data based on the data index. Results indicated good agreement between model output and experimental data.

In Figure 5, the estimations obtained are compared with the actual measured data. Based on the Figure 5, the estimated data and experimental measurements have an acceptable closeness.

In Figure 6, the relative deviation for the GMDH model applied for effective thermal conductivity is represented. As shown in Figure 6, ARD decreases and

reaches zero for effective thermal conductivity higher than 10,000 W/K.m.

Results obtained from the model for effective thermal conductivity are compared with experimental data in Figure 7. As shown, there is good agreement between experimental data and data obtained from the model. The model is more suitable at higher effective thermal conductivity.

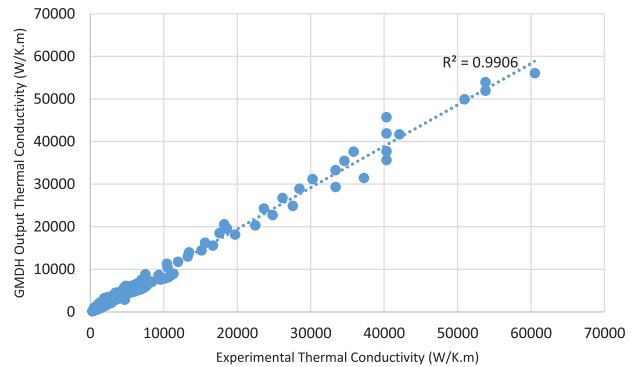


Figure 7. GMDH estimation versus actual data of effective thermal conductivity.

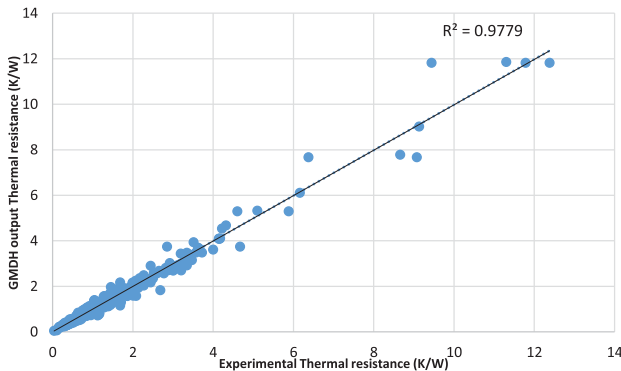


Figure 5. GMDH estimation versus actual data of thermal resistance.

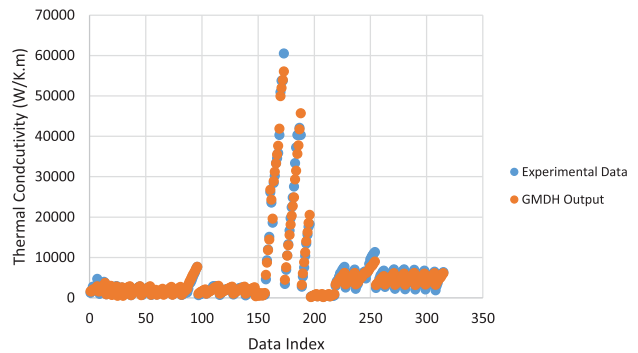


Figure 8. GMDH output versus actual data of effective thermal conductivity on the basis of the data index.

Results of the GMDH technique employed are shown in Figure 8 in order to evaluate the effective thermal conductivity of PHPs based on their data index.

4. Conclusion

A novel method to determine the thermal resistance and effective thermal conductivity of PHPs filled with water as working fluid has been presented. The technique utilizes GMDH in order to obtain an applicable route for calculating the thermal resistance and effective thermal conductivity of PHPs. Accurate experimental data are extracted from valid studies. Results indicate that the GMDH method is an appropriate tool for predicting heat transfer characteristics of PHPs with low degree of uncertainty.

Since GMDH shows a favorable performance in estimating PHPs' thermal behavior, other ANN-based models with various algorithms can be tested to evaluate their performance. Moreover, different machine learning approaches such as support vector machine-based models can be evaluated in estimating the thermal performance of PHPs. Coupling various optimization algorithms with machine learning methods is another idea to minimize the deviation of the models and achieve higher accuracy. Finally, according to the acceptable precision of the current model, this approach can be applied to PHPs filled with various operating fluids such as ethanol, acetone, etc.

Nomenclature

l_a	length of adiabatic section
l_c	length of condenser section
l_e	length of evaporator section
l_{eff}	effective length
d_i	inner diameter
d_o	outer diameter
K	thermal conductivity of heat pipe
q	heat input
R	thermal resistance of heat pipe

Disclosure statement

No potential conflict of interest was reported by the authors.

References

- Ahmadi, M. H., Ahmadi, M. A., Mehrpooya, M., & Rosen, M. A. (2015). Using GMDH neural networks to model the power and torque of a stirling engine. *Sustainability (Switzerland)*, 7(2), 2243–2255. doi:10.3390/su7022243
- Alhuyi Nazari, M., Ahmadi, M. H., Ghasempour, R., & Shafii, M. B. (2018). How to improve the thermal performance of pulsating heat pipes: A review on working fluid. *Renewable and Sustainable Energy Reviews*, 91, 630–638.
- Ali Ahmadi, M., & Golshadi, M. (2012). Neural network based swarm concept for prediction asphaltene precipitation due to natural depletion. *Journal of Petroleum Science and Engineering*, 98–99, 40–49. doi:10.1016/j.petrol.2012.08.011
- Alizadeh, H., Ghasempour, R., Shafii, M. B., Ahmadi, M. H., Yan, W.-M., & Nazari, M. A. (2018). Numerical simulation of PV cooling by using single turn pulsating heat pipe. *International Journal of Heat and Mass Transfer*, 127, 203–208. doi:10.1016/J.IJHEATMASTRANSFER.2018.06.108
- Baghban, A., Jalali, A., Shafiee, M., Ahmadi, M. H., & Chau, K. (2019). Developing an ANFIS-based swarm concept model for estimating the relative viscosity of nanofluids. *Engineering Applications of Computational Fluid Mechanics*, 13(1), 26–39. doi:10.1080/19942060.2018.1542345
- Bildirici, M., & Ersin, Ö. (2014). Modeling Markov switching ARMA-GARCH neural networks models and an application to forecasting stock returns. *The Scientific World Journal*, 2014, 1–21. doi:10.1155/2014/497941
- Buffone, C., Sefiane, K., Buffone, L., & Lin, S. (2005). Heat transfer enhancement in heat pipe applications using surface coating. *Journal of Enhanced Heat Transfer*, 12(1), 21–36. doi:10.1615/JEnhHeatTransf.v12.i1.20
- Cui, X., Zhu, Y., Li, Z., & Shun, S. (2014). Combination study of operation characteristics and heat transfer mechanism for pulsating heat pipe. *Applied Thermal Engineering*, 65(1–2), 394–402. doi:10.1016/j.applthermaleng.2014.01.030
- Daimaru, T., Yoshida, S., & Nagai, H. (2017). Study on thermal cycle in oscillating heat pipes by numerical analysis. *Applied Thermal Engineering*, 113, 1219–1227. doi:10.1016/J.APPLTHERMALENG.2016.11.114
- Ebrahimi, M., Shafii, M. B., & Bijarchi, M. A. (2015). Experimental investigation of the thermal management of flat-plate closed-loop pulsating heat pipes with interconnecting channels. *Applied Thermal Engineering*, 90, 838–847. doi:10.1016/J.APPLTHERMALENG.2015.07.040
- Elçiçek, H., Akdoğan, E., & Karagöz, S. (2014). The use of artificial neural network for prediction of dissolution kinetics. *The Scientific World Journal*, 2014, 1–9. doi:10.1155/2014/194874
- Faghri, A. (1995). *Heat pipe science and technology*. Taylor & Francis. Retrieved from <https://books.google.com/books?hl=en&lr=&id=9QpQAQAQBAJ&oi=fnd&pg=PR15&dq=heat+pipe+science&ots=MRzBSXtSOg&sig=l-z27OGf9Yvxpriuvjbl7Gw9T0I#v=onepage&q=heat+pipe+science&f=false>
- Faizollahzadeh Ardabili, S., Najafi, B., Shamshirband, S., Minaei Bidgoli, B., Deo, R. C., & Chau, K. (2018). Computational intelligence approach for modeling hydrogen production: A review. *Engineering Applications of Computational Fluid Mechanics*, 12(1), 438–458. doi:10.1080/19942060.2018.1452296
- Farlow, S. J., & Farlow, J. S. (1984). *Self-organizing methods in modeling: GMDH-type algorithms*. M. Dekker. Retrieved from <https://dl.acm.org/citation.cfm?id=537766>
- Gandomkar, A., Saidi, M. H., Shafii, M. B., Vandadi, M., & Kalan, K. (2017). Visualization and comparative investigations of pulsating ferro-fluid heat pipe. *Applied Thermal Engineering*, 116, 56–65. doi:10.1016/J.APPLTHERMALENG.2017.01.068

- Gonzalez-Sanchez, A., Frausto-Solis, J., & Ojeda-Bustamante, W. (2014). Attribute selection impact on linear and non-linear regression models for crop yield prediction. *The Scientific World Journal*, 2014, 509429. doi:10.1155/2014/509429
- Hemmat Esfe, M., Tatar, A., Ahangar, M. R. H., & Rostamian, H. (2018). A comparison of performance of several artificial intelligence methods for predicting the dynamic viscosity of TiO₂/SAE 50 nano-lubricant. *Physica E: Low-Dimensional Systems and Nanostructures*, 96, 85–93. doi:10.1016/j.physe.2017.08.019
- Ivakhnenko, A. G. (1971). Polynomial theory of complex systems. *IEEE Transactions on Systems, Man, and Cybernetics*, SMC-1(4), 364–378. doi:10.1109/TSMC.1971.4308320
- Jamali, A., Nariman-Zadeh, N., Darvizeh, A., Masoumi, A., & Hamrang, S. (2009). Multi-objective evolutionary optimization of polynomial neural networks for modelling and prediction of explosive cutting process. *Engineering Applications of Artificial Intelligence*, 22(4–5), 676–687. doi:10.1016/j.engappai.2008.11.005
- Jia, H., Jia, L., & Tan, Z. (2013). An experimental investigation on heat transfer performance of nanofluid pulsating heat pipe. *Journal of Thermal Science*, 22(5), 484–490. doi:10.1007/s11630-013-0652-8
- Li, J., & Yan, L. (2008). Experimental research on heat transfer of pulsating heat pipe. *Journal of Thermal Science*, 17(2), 181–185. doi:10.1007/s11630-008-0181-z
- Lin, J.-Y., Cheng, C.-T., & Chau, K.-W. (2006). Using support vector machines for long-term discharge prediction. *Hydrological Sciences Journal*, 51(4), 599–612. doi:10.1623/hysj.51.4.599
- Lin, Y. H., Kang, S. W., & Chen, H. L. (2008). Effect of silver nano-fluid on pulsating heat pipe thermal performance. *Applied Thermal Engineering*, 28(11–12), 1312–1317. doi:10.1016/j.applthermaleng.2007.10.019
- Mameli, M., Manno, V., Filippeschi, S., & Marengo, M. (2014). Thermal instability of a closed loop pulsating heat pipe: Combined effect of orientation and filling ratio. *Experimental Thermal and Fluid Science*, 59, 222–229. doi:10.1016/j.expthermflusci.2014.04.009
- Moazenzadeh, R., Mohammadi, B., Shamshirband, S., & Chau, K. (2018). Coupling a firefly algorithm with support vector regression to predict evaporation in northern Iran. *Engineering Applications of Computational Fluid Mechanics*, 12(1), 584–597. doi:10.1080/19942060.2018.1482476
- Mohammadi, M., Mohammadi, M., & Shafii, M. B. (2012). Experimental investigation of a pulsating heat pipe using ferrofluid (magnetic nanofluid). *Journal of Heat Transfer*, 134(1), 014504. doi:10.1115/1.4004805
- Motahar, S., & Khodabandeh, R. (2016). Experimental study on the melting and solidification of a phase change material enhanced by heat pipe. *International Communications in Heat and Mass Transfer*, 73, 1–6. doi:10.1016/j.icheatmasstransfer.2016.02.012
- Nariman-zadeh, N., Atashkari, K., Jamali, A., Pilechi, A., & Yao, X. (2005). Inverse modelling of multi-objective thermodynamically optimized turbojet engines using GMDH-type neural networks and evolutionary algorithms. *Engineering Optimization*, 37(5), 437–462. doi:10.1080/0305215050035591
- Nariman-Zadeh, N., Darvizeh, A., Felezi, M. E., & Gharababaei, H. (2002). Polynomial modelling of explosive compaction process of metallic powders using GMDH-type neural networks and singular value decomposition. *Modelling and Simulation in Materials Science and Engineering*, 10(6), 727–744. doi:10.1088/0965-0393/10/6/308
- Nazari, M. A., Ghasempour, R., Ahmadi, M. H., Heydari, G., & Shafii, M. B. (2018). Experimental investigation of graphene oxide nanofluid on heat transfer enhancement of pulsating heat pipe. *International Communications in Heat and Mass Transfer*, 91, 90–94. doi:10.1016/j.icheatmasstransfer.2017.12.006
- Qu, J., & Wang, Q. (2013). Experimental study on the thermal performance of vertical closed-loop oscillating heat pipes and correlation modeling. *Applied Energy*, 112, 1154–1160. doi:10.1016/j.apenergy.2013.02.030
- Ramezanizadeh, M., Ahmadi, M. A., Ahmadi, M. H., & Alhuyi Nazari, M. (2018). Rigorous smart model for predicting dynamic viscosity of Al₂O₃/water nanofluid. *Journal of Thermal Analysis and Calorimetry*, 1, doi:10.1007/s10973-018-7916-1
- Ramezanizadeh, M., Nazari, M. A., Ahmadi, M. H., Lorenzini, G., Kumar, R., & Jilte, R. (n.d.). A review on the solar applications of thermosyphons. *Mathematical Modelling of Engineering Problems*, 5(4), 275–280. doi:10.18280/mmep.050401
- Rezaei, M. H., Sadeghzadeh, M., Alhuyi Nazari, M., Ahmadi, M. H., & Astarai, F. R. (2018). Applying GMDH artificial neural network in modeling CO₂ emissions in four nordic countries. *International Journal of Low-Carbon Technologies*, doi:10.1093/ijlct/cty026
- Saha, N., Das, P. K., & Sharma, P. K. (2014). Influence of process variables on the hydrodynamics and performance of a single loop pulsating heat pipe. *International Journal of Heat and Mass Transfer*, 74, 238–250. doi:10.1016/j.ijheatmasstransfer.2014.02.067
- Shafii, M. B., Arabnejad, S., Saboohi, Y., & Jamshidi, H. (2010). Experimental investigation of pulsating heat pipes and a proposed correlation. *Heat Transfer Engineering*, 31(10), 854–861. doi:10.1080/01457630903547636
- Taormina, R., Chau, K.-W., & Sivakumar, B. (2015). Neural network river forecasting through baseflow separation and binary-coded swarm optimization. *Journal of Hydrology*, 529, 1788–1797. doi:10.1016/j.jhydrol.2015.08.008
- Wang, S., Lin, Z., Zhang, W., Chen, J., & Tang, Y. (2009). Heat transport characteristics of an oscillating heat pipe with Al. In *ASME 2009 second international conference on micro/nanoscale heat and mass transfer, volume 3* (pp. 331–335). ASME. doi:10.1115/MNHMT2009-18530.
- Wang, J., Ma, H., Zhu, Q., Dong, Y., & Yue, K. (2016). Numerical and experimental investigation of pulsating heat pipes with corrugated configuration. *Applied Thermal Engineering*, 102, 158–166. doi:10.1016/j.applthermaleng.2016.03.163
- Wu, C. L., & Chau, K. W. (2011). Rainfall-runoff modeling using artificial neural network coupled with singular spectrum analysis. *Journal of Hydrology*, 399(3–4), 394–409. doi:10.1016/j.jhydrol.2011.01.017
- Yao, X. (1999). Evolving artificial neural networks. *Proceedings of the IEEE*, 87(9), 1423–1447. doi:10.1109/5.784219

- Yaseen, Z. M., Sulaiman, S. O., Deo, R. C., & Chau, K.-W. (2019). An enhanced extreme learning machine model for river flow forecasting: State-of-the-art, practical applications in water resource engineering area and future research direction. *Journal of Hydrology*, 569, 387–408. doi:10.1016/j.jhydrol.2018.11.069
- Zamani, R., Kalan, K., & Shafii, M. B. (2018). Experimental investigation on thermal performance of closed loop pulsating heat pipes with soluble and insoluble binary working fluids and a proposed correlation. *Heat and Mass Transfer*, 1–10. doi:10.1007/s00231-018-2418-z
- Zhao, N., Zhao, D., & Ma, H. (2013). Experimental investigation of magnetic field effect on the magnetic nanofluid oscillating heat pipe. *Journal of Thermal Science and Engineering Applications*, 5(1), 011005. doi:10.1115/1.4007498
- Zhu, Y., Cui, X., Han, H., & Sun, S. (2014). The study on the difference of the start-up and heat-transfer performance of the pulsating heat pipe with water-acetone mixtures. *International Journal of Heat and Mass Transfer*, 77, 834–842. doi:10.1016/j.ijheatmasstransfer.2014.05.042